A bipolar analytical and parametric finite element method analysis of surface loading in semi-infinite mass with a circular opening

ARTICLE *in* MATHEMATICAL MODELLING · DECEMBER 1982

DOI: 10.1016/0270-0255(82)90029-X

3 AUTHORS, INCLUDING:

Mehmet T. Tumay

Louisiana State University

72 PUBLICATIONS **494** CITATIONS

Mathematical Modelling, Vol. 3, pp. 259–278
Printed in the USA.

0270-0255/82/030259-20$03.00/0

A BIPOLAR ANALYTICAL AND PARAMETRIC FINITE ELEMENT METHOD ANALYSIS OF SURFACE LOADING IN SEMI-INFINITE MASS WITH A CIRCULAR OPENING

YALCIN B. ACAR
Department of Civil Engineering
Louisiana State University
Baton Rouge, Louisiana 70803, USA

H. T. DURGUNOGLU
Department of Civil Engineering
Bogazici University
Bebek, Istanbul, Turkey

MEHMET T. TUMAY
Department of Civil Engineering
Louisiana State University
Baton Rouge, Louisiana 70803, USA

Communicated by Xavier J. R. Avula

Abstract—A closed form elasticity solution to stresses and displacements around a circular opening in semi-infinite mass with infinite, uniform surface loading is presented with the use of the bipolar coordinate system. The arrangement of the stress tensor and the displacement vector in bipolar coordinates, together with the transformation matrices is also provided. The results are numerically evaluated, and comparisons are made with previous infinite medium solutions. The case of variable loading width at the surface and the effect of rigid base is parametrically analyzed by the finite element method for stresses and surface displacements. The basic implications to engineering analyses are discussed. It is concluded that while analytical procedure easily provide solutions to the generalized problem, cases involved with difficult boundary conditions can only be analyzed by mathematical modelling of the medium and using a proper numerical procedure such as the finite element method.

1. INTRODUCTION

The rapid industrialization together with social and urban development brings the need for construction of various kinds of underground structures such as transportation tunnels or large diameter conduits. In the design of these underground structures, engineering analysis and a careful prediction of loads and displacements around subsurface openings are essential for a proper design.

The accurate analysis of loads about openings requires a primary knowledge of the stresses induced about these openings by different gravitational forces or boundary loadings. The types of pressure that are exerted upon the underground structures could be classified as the loosening pressures of the subsurface formation, overburden pressures, swelling pressures, or pressures induced by exterior loadings.

Although the engineering properties of the subsurface formation and the basic geological discontinuities govern the types of pressure to be encountered in soil and rock masses, whenever the boundary conditions permit, the theory of elasticity provides the analytical tool to a large number of problems that have direct and indirect applications.

In cases of complicated loading and boundary conditions, however, numerical methods with proper discretization of the medium prevails. The distribution of stress, strain and displacements disturbed by the excavation of a tunnel and developing around the excavated opening are previously studied by various investigators [1–7]. Furthermore, the solution for the analytical determination of stresses developing around a circular opening, in semi-infinite medium under geostatic forces, is given [8].

In review of the previous investigations on circular openings in infinite and semi-infinite mass, it is observed that the elastic solution to the case of a single circular opening in semi-infinite mass with uniform surface loading, has not been thoroughly investigated. Practical applications of this case arise in engineering applications when an embankment, fill, or superstructure is to be built over an already existing opening which is close to the surface of the semi-infinite medium. In such cases of problems, it is also important to estimate the amount of differential surface displacements in order to meet the settlement criteria of the superstructure. The need for analysis of stresses and displacements around underground openings in these cases is the main purpose of the study presented. The investigations are confined to only circular openings due to the vast extent and scope of the work.

2. STRESS CONDITIONS AROUND CIRCULAR AND ELLIPTICAL OPENINGS IN INFINITE MASS

The classical problem of an opening in a plate subjected to a uniaxial stress is given by Timoshenko and Goodier [9]. However, the problem of determining the stress conditions in a rock about circular and elliptical cavities an infinite mass was first studied by Terzaghi and Richart [7].

Stress conditions around circular openings subject to geostatic forces was first investigated by Mindlin [8]. Since there does not exist any theoretical method to predict the magnitude of horizontal pressures in the rock, three cases of *in situ* stresses were postulated; namely, the hydrostatic pressure condition, the case of confined lateral deformation and the case of no lateral pressure [10]. In the solution of the problem, Mindlin [8] used the bipolar coordinate system of Jeffrey [10], where the plane stress and plane strain problems in bipolar coordinates are discussed. In a discussion given to Mindlin's analytical solution, Brahtz [11] pointed out the fact that the practical cases of loading include the cases when the straight or circular boundaries are subjected to loads. In this discussion, the theoretical solution when uniform normal loads are applied on all external boundaries is also presented. However, when the openings are close to the surface and when only the ground surface is loaded, there does not exist any other loading on the vertical boundaries. Consequently, the solution for a circular tunnel in semi-infinite elastic media and loaded only on the horizontal straight boundary should be determined and analyzed.

In the case of uniform, infinite surface loading, the analytical solution to stresses and displacements could be solved without any difficulty by a transformation into bipolar coordinates. The case of parametric study of finite loading, however, needs proper modelling of the medium and solution with numerical procedures such as the finite element method.

3. ANALYTICAL SOLUTION IN BIPOLAR COORDINATE SYSTEM

It is intended to obtain the solution for stresses and deformations around an unlined circular underground opening in semi-infinite elastic half-space and uniformly loaded at the surface. This plane strain problem is illustrated in Fig. 1.

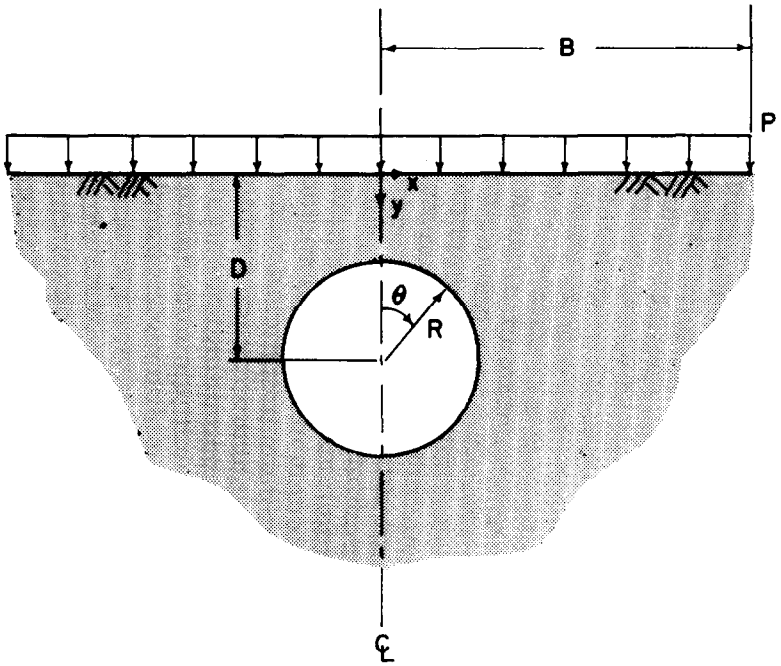

Fig. 1. Unlined circular opening with uniform infinite loading at the surface.

It is necessary to ease the solution by adoption of a proper curvilinear coordinate system. Therefore, the bipolar coordinate system presented in Fig. 2 and which is frequently used in the solution of similar problems is chosen. The transformation of Cartesian coordinates to bipolar coordinates is given by

$$x = \frac{a \sin\beta}{\cosh\alpha - \cos\beta} \tag{1a}$$

$$y = \frac{a \sinh\alpha}{\cosh\alpha - \cos\beta}. \tag{1b}$$

The components of displacements in bipolar coordinates are found in terms of a normalized Airy–Stress function h_χ {where $h_\chi = h(\chi/h)$ and h is the metric tensor [10, 12]} and another function Q which is derived from h_χ as

$$2\mu v = \frac{\mu}{\lambda+\mu}\left\{\frac{\partial(h\chi)}{\partial\alpha} - \frac{\sinh\alpha}{\cosh\alpha-\cos\beta}h_\chi\right\} - \left\{\frac{\partial(hQ)}{\partial\beta} - \frac{\sin\beta}{\cosh\alpha-\cos\beta}hQ\right\} \tag{2a}$$

$$2\mu u = \frac{\mu}{\lambda+\mu}\left\{\frac{\partial(h\chi)}{\partial\beta}\frac{\sin\beta}{\cosh\alpha-\cos\beta}h_\chi\right\} + \left\{\frac{\partial(hQ)}{\partial\beta} - \frac{\sinh\alpha}{\cosh\alpha-\cos\beta}hQ\right\}, \tag{2b}$$

where hQ is defined as

$$hQ = \frac{\lambda+2\mu}{2(\lambda+\mu)}\int\int\left\{\frac{\partial^2(h)}{\partial\alpha^2}\frac{\partial^2(h)}{\partial\beta^2} - h_\chi\right\}d\alpha\,d\beta + hQ_1 \tag{2c}$$

and λ, μ are the Lame's constants. The values of Q_1 would give rise in u and v corresponding to motions of pure translation and rigid body rotation about the origin.

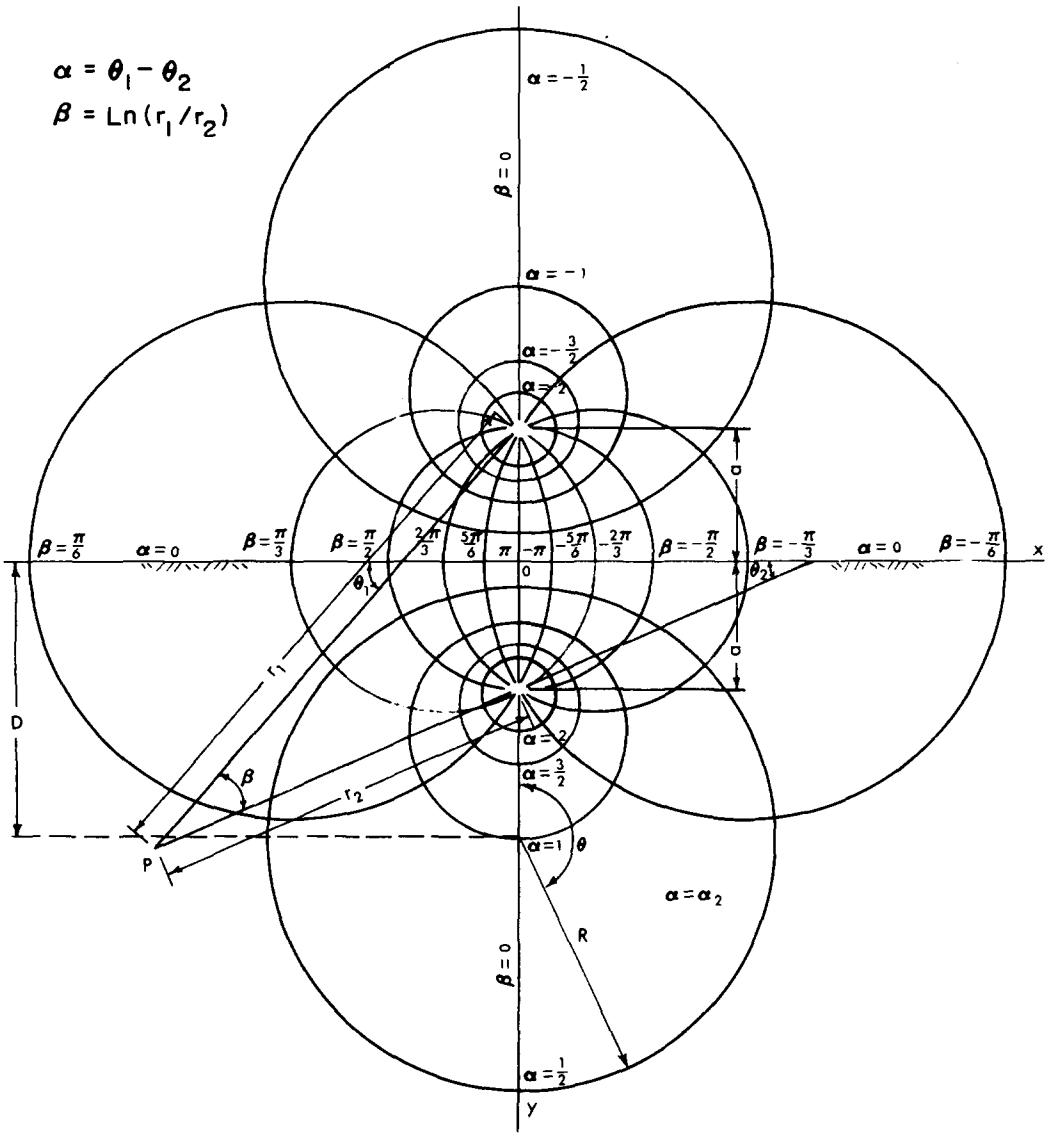

Fig. 2. Bipolar coordinate system.

In the solution of this second boundary value problem of elasticity, application of all the restrictions on the Airy–Stress function obtained through the solution of a linear differential equation with constant coefficients [13] would give the final form of the stress function h_χ as

$$h_\chi = aP\left\{\frac{1}{2}\sinh\alpha\left(1+2\sum_{2}^{\infty}e^{-n\alpha}\cos n\beta\right) - D\sinh\alpha + B_0\alpha\cosh\alpha + [B_0\sinh\alpha\cosh\alpha - B_0\alpha + A_1\cosh 2\alpha + B_1]\cos\beta + \sum_{2}^{\infty}\phi_n(\alpha)\cos n\beta\right\}, \tag{3}$$

where

$$B_0 = \frac{\sinh\alpha_2 - 2\cosh\alpha_2}{2\sinh^3\alpha_2} \tag{4a}$$

$$A_1 = \frac{1}{2}\left[\frac{1 - e^{-\alpha_2}\sinh\alpha_2}{\sinh^2\alpha_2}\right] \tag{4b}$$

$$B_1 = \frac{1}{2}\left[\frac{1 - 2\cosh^2\alpha_2 + e^{-\alpha_2}\sinh\alpha_2}{\sinh^2\alpha_2}\right] \tag{4c}$$

$$D = \frac{1}{2\sinh^2\alpha_2} \tag{4d}$$

and

$$\Phi_n(\alpha) = A_n[\cosh(n+1)\alpha - \cosh(n-1)\alpha] + E_n[(n-1)\sinh(n+1)\alpha - (n+1)\sinh(n-1)\alpha] \tag{4e}$$

$$A_n = -\frac{n^2\sinh^2\alpha_2 - n\sinh\alpha_2\cosh\alpha_2 + e^{-n\alpha_2}\sinh n\alpha_2}{2(\sinh^2 n\alpha_2 - n^2\sinh^2\alpha_2)} \tag{4f}$$

$$E_n = \frac{n\sinh^2\alpha_2}{2(\sinh^2 n\alpha_2 - n^2\sinh^2\alpha_2)}, \tag{4g}$$

where $\alpha = \alpha_2$ represents the coordinate of the circular opening in Fig. 2. With the use of the stress function, the stresses in bipolar coordinates could be obtained by direct differentiation,

$$\begin{aligned}\sigma_{\alpha\alpha} = {} & A_1\cosh 2\alpha + B_1 - \sinh\alpha\sin\beta(B_0\cosh 2\alpha - B_0 + 2A_1\sinh 2\alpha) \\ & + (\cosh\alpha - \cos\beta)\left(-\sinh\alpha\sum_1^\infty n^2 e^{-n\alpha}\cos n\beta - \sum_1^\infty \Phi_n n^2\cos n\beta\right) \\ & - \sinh\alpha\left(-\sinh\alpha\sum_1^\infty n\, e^{-n\alpha}\cos n\beta + \sum_2^\infty \phi_n'(\alpha)\cos n\beta\right) \\ & + \sin\beta\left(\sinh\alpha\sum_1^\infty n\, e^{-n\alpha}\sin n\beta + \sum_2^\infty \Phi_n(\alpha) n\sin n\beta\right) \\ & + \cosh\alpha\left(\sum_2^\infty \phi_n(\alpha)\cos n\beta\right)\end{aligned} \tag{5a}$$

$$\begin{aligned}\sigma_{\beta\beta} = {} & B_0\sinh 2\alpha + A_1\cosh 2\alpha + B_1 + 4\cos\beta(\cosh\alpha - \cos\beta)(B_0\cosh\alpha\sinh\alpha + A_1\cosh 2\alpha) \\ & - \sinh\alpha\cos\beta(B_0\cosh 2\alpha + 2A_1\sinh 2\alpha + B_0) + (\cosh\alpha - \cos\beta) \\ & \times\left(\sum_2^\infty \phi_n''(\alpha)\cos n\beta - 2\cosh\alpha\sum_1^\infty n\, e^{-n\alpha}\cos n\beta + \sinh\alpha\sum_1^\infty n^2 e^{-n\alpha}\cos n\beta\right) \\ & - \sinh\alpha\left(\sum_2^\infty \phi_n'(\alpha)\cos n\beta - \sinh\alpha\sum_1^\infty n\, e^{-n\alpha}\cos n\beta\right) \\ & + \sin\beta\left(\sum_2^\infty \Phi_n(\alpha) n\sin n\beta + \sinh\alpha\sum_1^\infty n\, e^{-n\alpha}\sin n\beta\right) \\ & + \cos\beta\left(\sum_2^\infty \Phi_n(\alpha)\cos n\beta\right)\end{aligned} \tag{5b}$$

$$\begin{aligned}\sigma_{\alpha\beta} = {} & (\cosh\alpha - \cos\beta)\Big\{\cosh\alpha\sum_1^\infty e^{-n\alpha} n\sin n\beta \\ & - \sinh\alpha\sum_1^\infty e^{-n\alpha} n^2\sin n\beta + \sum_2^\infty \Phi_n'(\alpha) n\sin n\beta \\ & + [B_0(\cosh 2\alpha - 1) + 2A_1\sinh 2\alpha]\sin\beta\Big\}.\end{aligned} \tag{5c}$$

The Fourier series expansions are valid for only $\alpha > 0$; therefore, the solution for $\alpha = 0$ which represents the ground surface should also be supplied. Converting the Fourier series, the solution for the surface of the semi-infinite half space could be found as

$$\sigma_{\alpha\alpha} = -1 \tag{6a}$$

$$\sigma_{\beta\beta} = (1 - \cos\beta)\left(4A_1 \cos\beta + 4\sum_{2}^{\infty} nA_n \cos n\beta\right) \tag{6b}$$

$$\sigma_{\alpha\beta} = 0. \tag{6c}$$

Equations (5) give the stresses in bipolar coordinates. The stress tensor in Cartesian coordinates could be obtained by the orthogonal coordinate transformation,

$$a_{ik} = \begin{bmatrix} \dfrac{-\sinh\alpha \sin\beta}{\cosh\alpha - \cos\beta} & \dfrac{\cosh\alpha \cos\beta - 1}{\cosh\alpha - \cos\beta} \\ \dfrac{1 - \cosh\alpha \cos\beta}{\cosh\alpha - \cos\beta} & \dfrac{-\sinh\alpha \sin\beta}{\cosh\alpha - \cos\beta} \end{bmatrix}. \tag{7}$$

The hQ function utilized for the solution of the displacements is obtained from Eqs. (2c) and (3) as

$$\begin{aligned} hQ = \frac{\lambda + \mu}{2(\lambda + 2\mu)} aP \Big\{ & -2 \sin\beta \left(\sum_{1}^{\infty} e^{-n\alpha} (\cos n\beta)\right) \\ & + 2B_0 \beta \cosh\alpha + (2A_1 \sinh 2\alpha + B_0 \cosh 2\alpha) \sin\beta \\ & + \sum_{2}^{\infty} 2\psi_n(\alpha) \sin n\beta \Big\}, \end{aligned} \tag{8a}$$

where

$$\begin{aligned} \phi_n(\alpha) = {} & A_n[\cosh(n+1)\alpha - \cosh(n-1)\alpha] \\ & + E_n[(n-1)\sinh(n+1)\alpha - (n+1)\sinh(n-1)\alpha] \end{aligned} \tag{8b}$$

$$\begin{aligned} \psi_n(\alpha) = {} & A_n[\sinh(n+1)\alpha - \sinh(n-1)\alpha] \\ & + E_n[(n-1)\cosh(n+1)\alpha - (n+1)\cosh(n-1)\alpha]. \end{aligned} \tag{8c}$$

The displacements in bipolar coordinates could now be found with the use of Eqs. (2) and (8) and the displacements in Cartesian coordinates with the use of the bipolar basis vectors would be

$$2\mu u_y = -v\left[\frac{\sinh\alpha \sin\beta}{\cosh\alpha - \cos\beta}\right] + u\left[\frac{\cosh\alpha \cos\beta - 1}{\cosh\alpha - \cos\beta}\right] - 2v_0 \tag{9a}$$

$$2\mu u_x = -v\left[\frac{\cosh\alpha \cos\beta - 1}{\cosh\alpha - \cos\beta}\right] + u\left[\frac{\sinh\alpha \sin\beta}{\cosh\alpha - \cos\beta}\right]. \tag{9b}$$

Since the strain tensor is stress dependent, the relations between stresses and strains are valid for any coordinate system. Furthermore, once the strains in bipolar coordinates are determined the orthogonal transformation matrix given by Eq. (7) could be used for the transformation to Cartesian coordinates.

4. NUMERICAL EVALUATIONS

The stress, strain, and displacement components can be normalized as

$$\sigma = I_\sigma P \tag{10a}$$

$$\epsilon = I_\epsilon \frac{P}{E} \tag{10b}$$

$$\delta_v = I_{\delta v} \frac{PR}{E}, \tag{10c}$$

where I_σ = stress influence ratio, I_ϵ = strain influence ratio, I_δ = displacement influence ratio, P = applied pressure, R = radius of the opening, E = deformation modulus, υ = Poisson's ratio, v = subscript for vertical displacement. The effect of the dimension of the circular opening could be eliminated by normalizing the Cartesian coordinates as x/R, y/R and the depth of the opening as D/R.

4.1. *Stresses*

The critical stresses occur due to the stress concentrations around the opening or at the surface as the opening approaches the surface. When the underground opening is far from the surface of the half-space, the problem converges to the limiting case of an unlined, circular opening in an infinite elastic space under uniform compression.

The tangential stress influence ratios, I_{σ_t}, at the surface of the opening is comparatively shown in Fig. 3. The limiting case of infinite D/R value is almost reached when this value is greater than three. Consequently, for D/R ratios of less than three, the location of the maximum tangential stress concentration around the opening tends to move towards the top, and also its value increasing without bound as D/R becomes equal to one. This change in the location and the value of the maximum tangential stress ratio with D/R, is presented in Fig. 4. It is again observed that adoption of the limiting case equations around the opening would almost correctly approximate the problem when D/R is greater than three.

Furthermore, as the opening approaches the surface of the semi-infinite half-space, the horizontal stresses on the ground surface become important. The variation of these stresses with x/R is given in Fig. 5 for different D/R values. It is observed that the maximum stress concentration is compressive and the location is on the symmetry axis at the surface. Horizontal stress concentrations at the surface are again negligible after a D/R value of three.

In order to comparatively illustrate the distribution of stresses along different vertical axes, a D/R value of 1.5 is chosen in Fig. 6. It is observed that pronounced differences from the limit case is valid for

$$y/R \leq D/R + 2.0 \tag{11a}$$

$$x/R \leq 5.0 \tag{11b}$$

$$D/R \leq 3.0. \tag{11c}$$

4.2. *Strains*

The evaluation of strains are important in determining the corresponding vertical or horizontal displacements when the deformation modulus, E, changes by depth or when

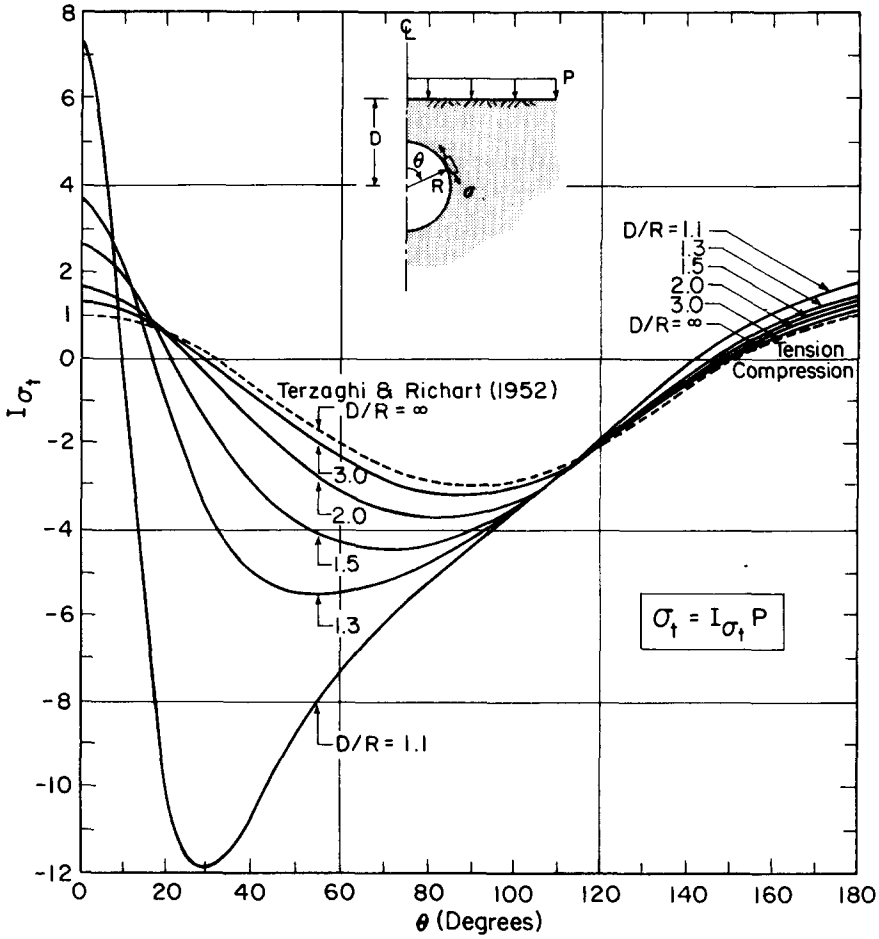

Fig. 3. Tangential stress ratios around the opening.

the half-space is layered. In such cases, direct integration of strain along a horizontal or vertical axis would give the specific horizontal or vertical displacements, respectively. The strain influence ratio, I_ϵ, is dependent on the Poisson's ratio, υ. The vital strains that should be considered are the ones along the vertical axes with x/R values of 0 and 1. These distributions of vertical strain ratios, $I\epsilon_\upsilon$, are presented in Fig. 7 for D/R values of 1.5, 2.0, 3.0 and at a Poisson's ratio of 0.25. It is observed that the strains around the opening increase and duely the deformation modulus around the opening is of vital importance. The settlements would increase if the opening is in a layer with lower deformation modulus. It should be added that in evaluation of displacements from strains on y axis there is a discontinuity in the material and the difference between the displacements of the crown and the bottom of the opening must be determined noting the discontinuity in the medium.

4.3. *Displacements*

The displacements are given as the relative displacements of any point with respect to the displacements at the origin ($x = 0.0$, $y = 0.0$). The vital displacements for engineering analysis would be the differential vertical surface settlements due to the infinite surface

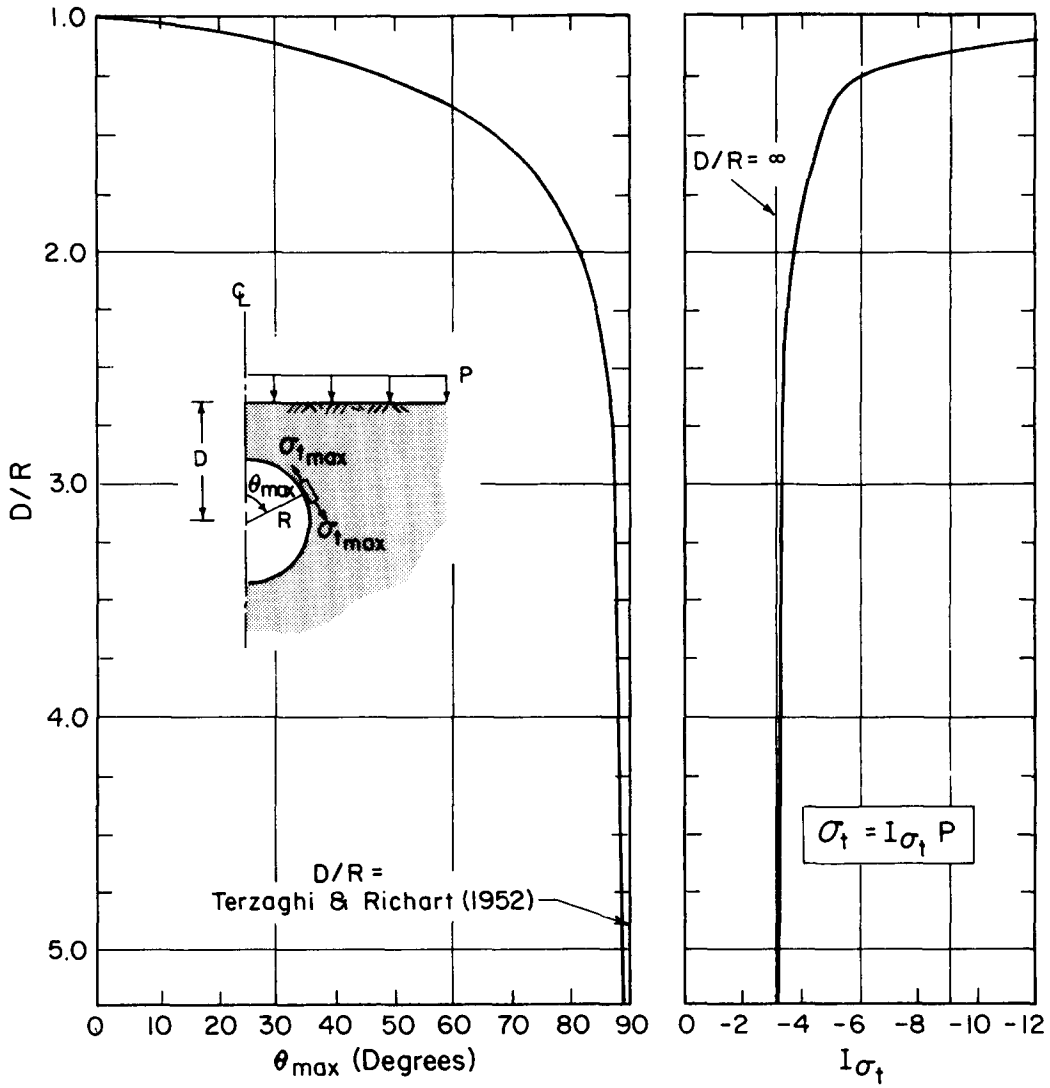

Fig. 4. The change of maximum tangential stress and location with D/R ratio.

loading of the semi-infinite elastic medium containing the unlined circular opening. Such cases could be encountered as the surface settlements under loads of fills when there exists large plastic conduits in the subsurface.

The influence ratios for differential settlements of the surface are presented for different D/R values in Fig. 8. It is also shown that the influence of the opening to the differential settlements at the surface is effective when

$$x/R \leq 2.0D/R. \tag{12}$$

Therefore, for any given D/R value, the differential settlements would be negligible for x/R values outside this range.

The variation of the surface settlements with the Poisson's ratio, are noted to be proportional to the quantity, $(1-\upsilon^2)$. Consequently, the surface settlements would be

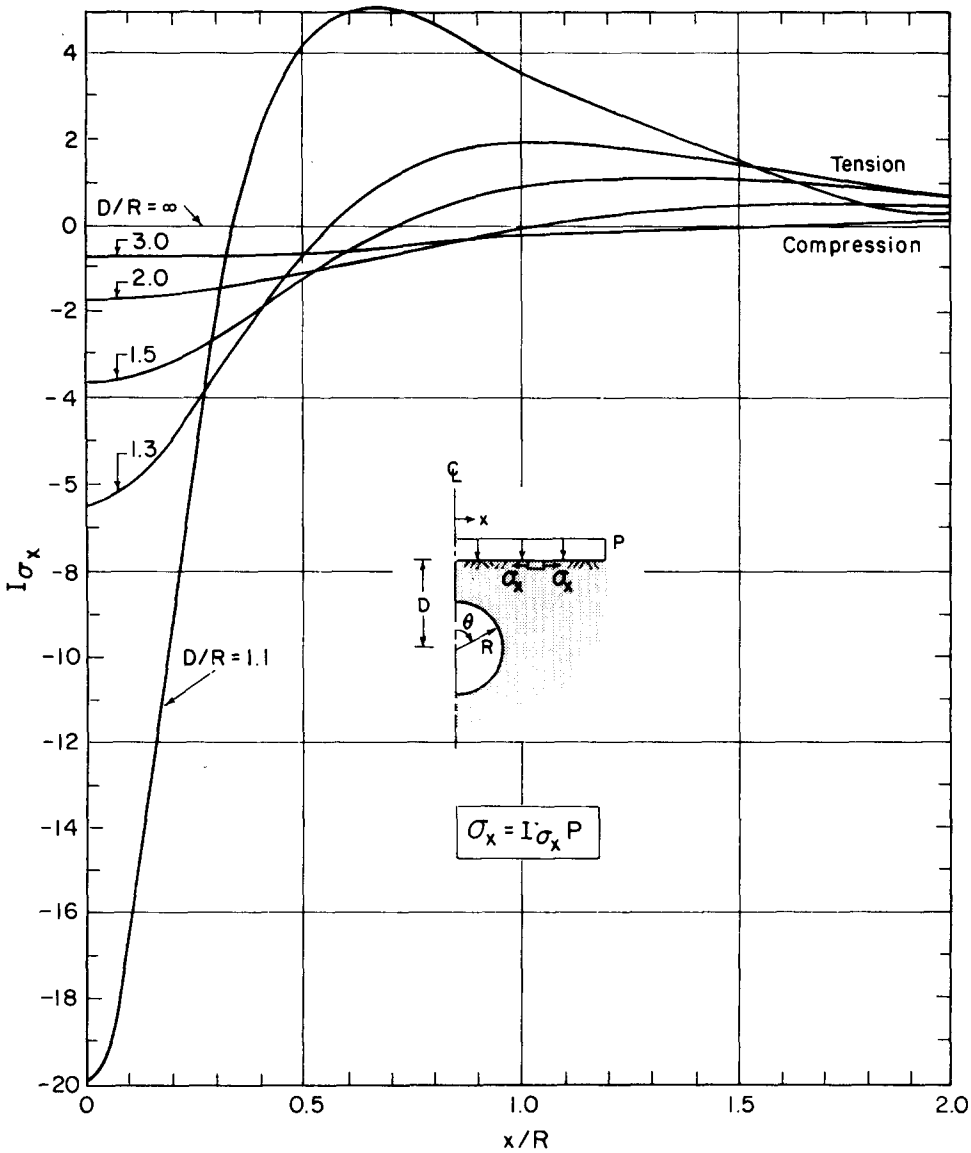

Fig. 5. Horizontal stress ratios at the half-space surface.

independent of the Poisson's ratio if they are normalized as

$$I_{\delta v} = \frac{E}{1-\upsilon^2}\frac{v}{PR}. \tag{13}$$

5. FINITE ELEMENT DISCRETIZATION

In the last decade, among the numerical methods for solutions of problems in engineering, finite element method (FEM) has extensively been favored [14]. In order to perform an accurate FEM analysis, proper discretization and modelling of the medium is necessary. To be able to analyze both a single circular opening and two circular openings

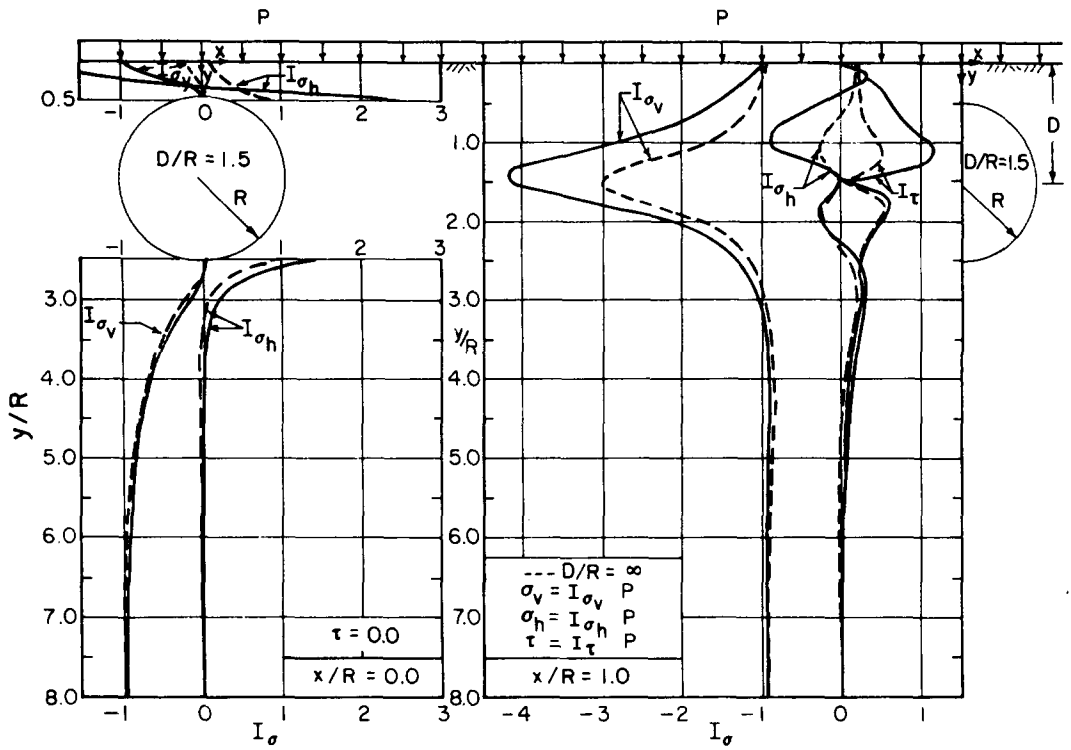

Fig. 6. Distribution of stresses along vertical axes ($D/R = 1.5$).

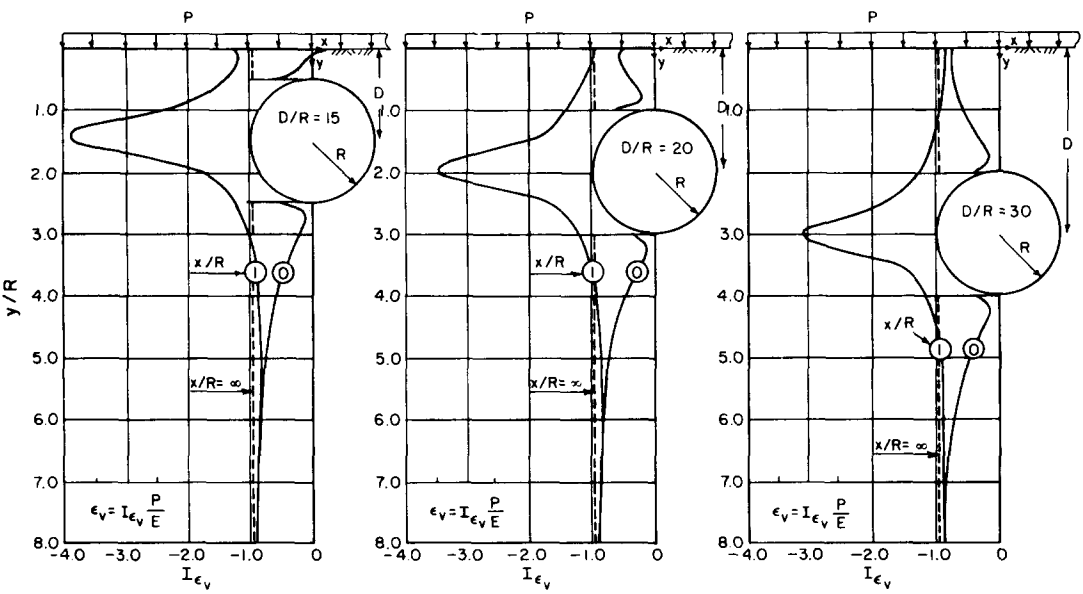

Fig. 7. Distribution of vertical strains for the Poisson ratio, $\nu = 0.25$.

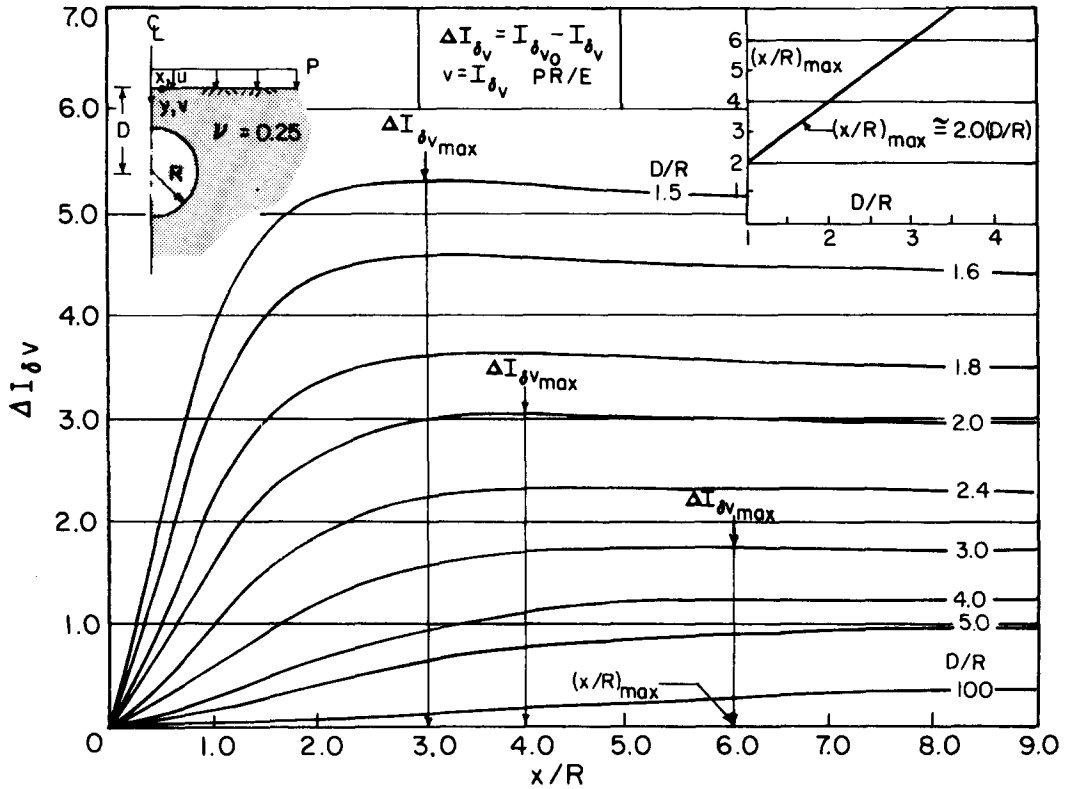

Fig. 8. Relative vertical surface displacements for $\nu = 0.25$.

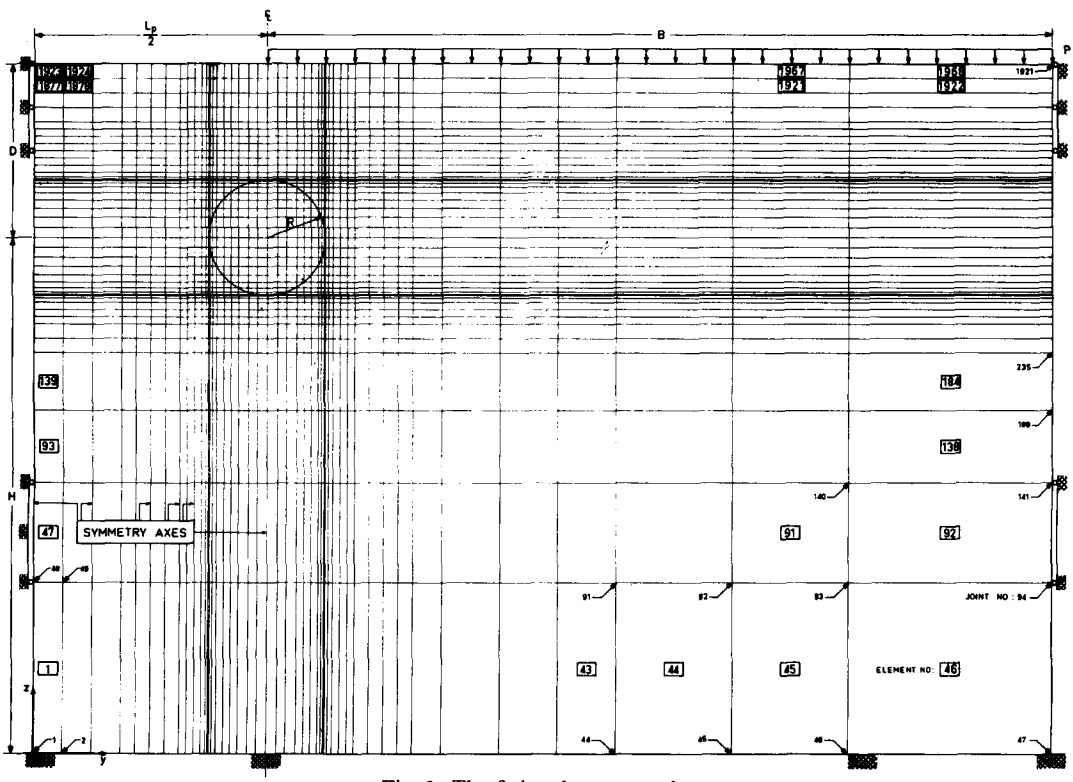

Fig. 9. The finite element mesh.

in semi-infinite, elastic half-space, the finite element mesh presented in Fig. 9 is constructed.

In the finite element method, it is necessary to represent the infinite medium by finite number of elements and this requires proper selection of vertical and horizontal distances from the opening. This dimensioning mainly depends upon the stresses and deformations induced by the loading. In the case of finite surface loading of a semi-infinite, half-space without any openings, taking $x/B = 8.5$, would suffice to represent the semi-infinite mass [15]. However, with respect to the vertical deformations, the semi-infinite medium is best represented when the vertical dimension of the mesh is chosen 18 times the minimum width of loading [16]. However, 6 times this half-width is found to be sufficient in analysis of the stresses [16, 17]. Similarly, in analysis of the problem of single or double openings in semi-infinite medium, the dimensioning of the mesh would be determined by B/R and H/R ratios. Consequently, in order to optimize the mesh and minimize the computer time required in solution of the problems, $x/R = 20.0$ and $H/R = 8.0$ were chosen to represent the semi-infinite media. The vertical boundary conditions at $x/R = 20.0$ were taken just as the conditions taken at the symmetry axis. The nodes at the rigid base is always restricted from both vertical and horizontal displacements. This would duely simulate a completely rough base.

The finite element method solutions were sought at constant deformation modulus, E, of 200,000 kg/cm^2 and constant Poisson's ratio of 0.25. However, the effect of Poisson's ratio was also investigated at values of $\upsilon = 0.0125$, 0.125, 0.25, 0.375, and 0.475. Since the finite element method solution is not stable for Poisson's ratio of 0.5, a value of 0.475 was used instead as the upper limit.

5.1. *Effect of the width of loading on the stresses*

The maximum stress concentrations occur around the opening and at the surface of the semi-infinite medium. The change of the tangential stresses, σ_t, around the opening is presented in Fig. 10 for a D/R value of 1.5. It is observed from this figure that the maximum stress concentration that occurs at the springings ($\theta = 90°$) of a circular opening in infinite medium moves toward the crown ($\theta = 0°$) and its value decreases as the width of loading decreases.

It is interesting to note that the tensile stresses at the crown is about $2.5p$ in the case of $B/R = 20.0$ and it drops to almost $0.5p$ when the loading width decreases to $B/R = 4.0$, however, this value increases to $0.8p$ as the loading width further decreases to $B/R = 1.0$. Hence, maximum tensile stress concentration occurs in the case of infinite loading and this value is almost reached for $B/R = 1.0$. Finite loading decreases the tensile stresses at the crown. The tensile stresses below the tunnel ($\theta = 180°$) obey the same rules; but, the value of the concentrations are much less than the crown.

The compressive stress concentrations are quite important due to the fact that stopping or popping will occur as a consequence of these stresses. It is observed that the maximum compressive stresses occur between the springings and the crown, its value increasing as the loading width increases and as the opening comes close to the surface.

The effect of opening depth on the location and value of the maximum tangential stress concentration is given in Fig. 11. The change is given for different B/R values. It is observed that when $D/R < 4.0$, the location of maximum stress concentration varies between $\theta = 65°$ to $\theta = 90°$ for different widths of loading. For any depth of the opening, this location could be determined from Fig. 11 at different B/R values. The respective values of the maximum stress concentrations are also provided in this figure. It is observed that the stress concentrations are very close to each other at $D/R = 1.5$ for B/R

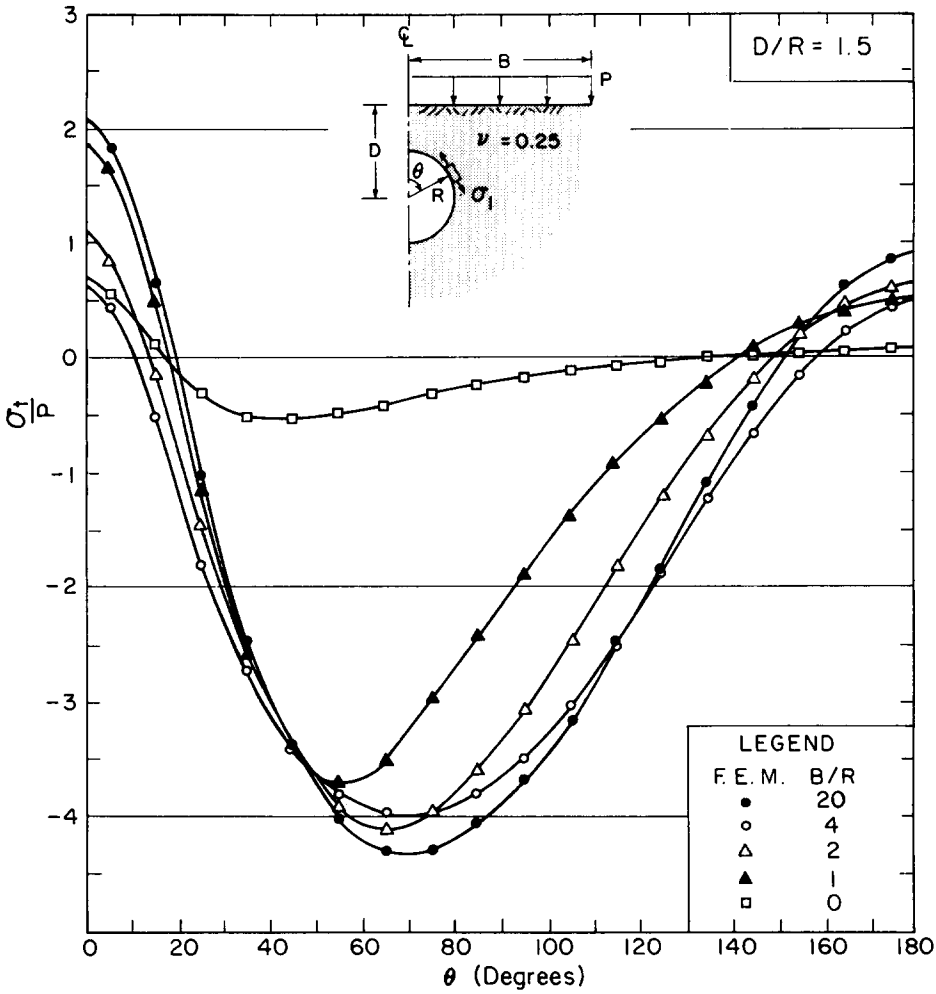

Fig. 10. The effect of the width of loading on tangential stresses around the opening ($D/R = 1.5$).

values of 1.0 to 20.0. The value decreases rapidly when B/R is less than 1.0. Furthermore, the maximum stress concentration is almost $1p$ when D/R is greater than 3.0 and B/R value is 1.0. This would indicate the fact that a superstructure, built at the surface with $B/R = 1.0$ and when $D/R > 4.0$, would increase the stresses just as much as the load superimposed at the surface.

A different version of Fig. 11 is presented in Fig. 12 as the change induced by the effect of loading on the location and value of maximum tangential stresses around the opening. This graph presents the location, θ_{max}, and value, σ_{max}, for different D/R values of 1.5, 2.0, and 3.0. It is possible to obtain θ_{max} and σ_{tmax} for any B/R or D/R value with the use of Figs. 11 and 12. In Fig. 12, it is noted that the shape of σ_{tmax}/P slightly changes for a D/R value of 1.5. When $D/R = 1.5$, the maximum stress concentration at $B/R = 1.0$ is about $4.2p$, which is greater than the value of $4.0p$ at $B/R = 20.0$. This is a clear indication that the effect of the straight boundary is felt for $D/R \leq 1.5$. In such cases, narrow widths of loading might increase the stress concentrations more than the limiting case of $B/R = 20.0$. However, it is also observed that when $B/R > 1.0$ and $D/R < 1.5$, the maximum stress concentration is very close to the limit case of $B/R = 20.0$ and therefore the value could closely be approximated by the analytical solution obtained.

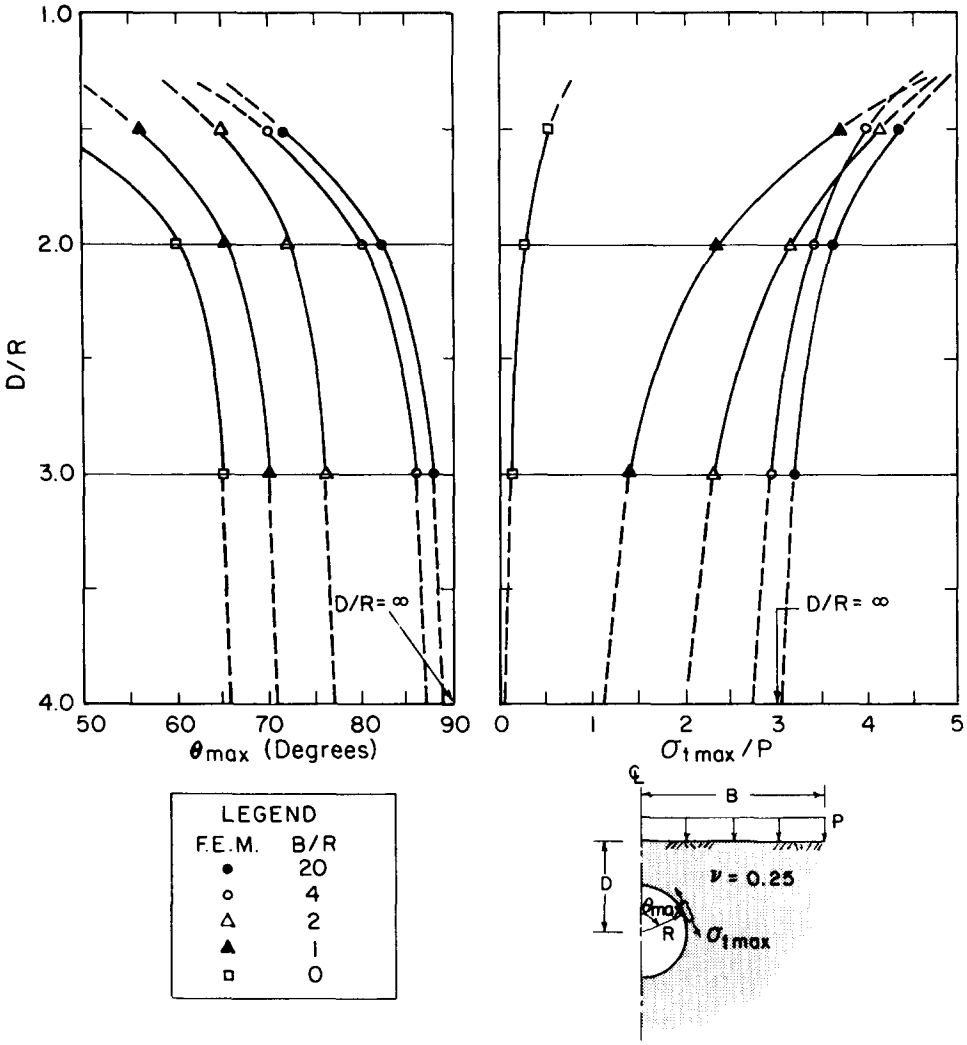

Fig. 11. The effect of opening depth on the location and value of the maximum tangential stress.

5.2. *Effect of the width of loading on surface displacements*

Theoretically, uniform, infinite loading of the ground surface would actually cause infinite settlements on a semi-infinite medium. Therefore, in evaluation of the surface displacements, the displacement of one point relative to the other is of value in engineering evaluations. Consequently, the differential settlements would be of question. In the case of finite loading it is possible to obtain the total settlements on the ground surface. The influence ratio $I_{\delta\upsilon}$ for total surface displacements are presented in Fig. 13 for D/R values of 1.5, 2.0, and 3.0. At each D/R value, the change of surface displacements are presented for loading width of $B/R = 0.0$, 1.0, 2.0, 4.0, and 20.0. It should be noted that finite loading on the surface favors differential settlements and extreme care should be taken in meeting the design criteria for settlement for structures to be built.

The displacements given in Fig. 13 is for a Poisson ratio of $\upsilon = 0.25$. The effect of

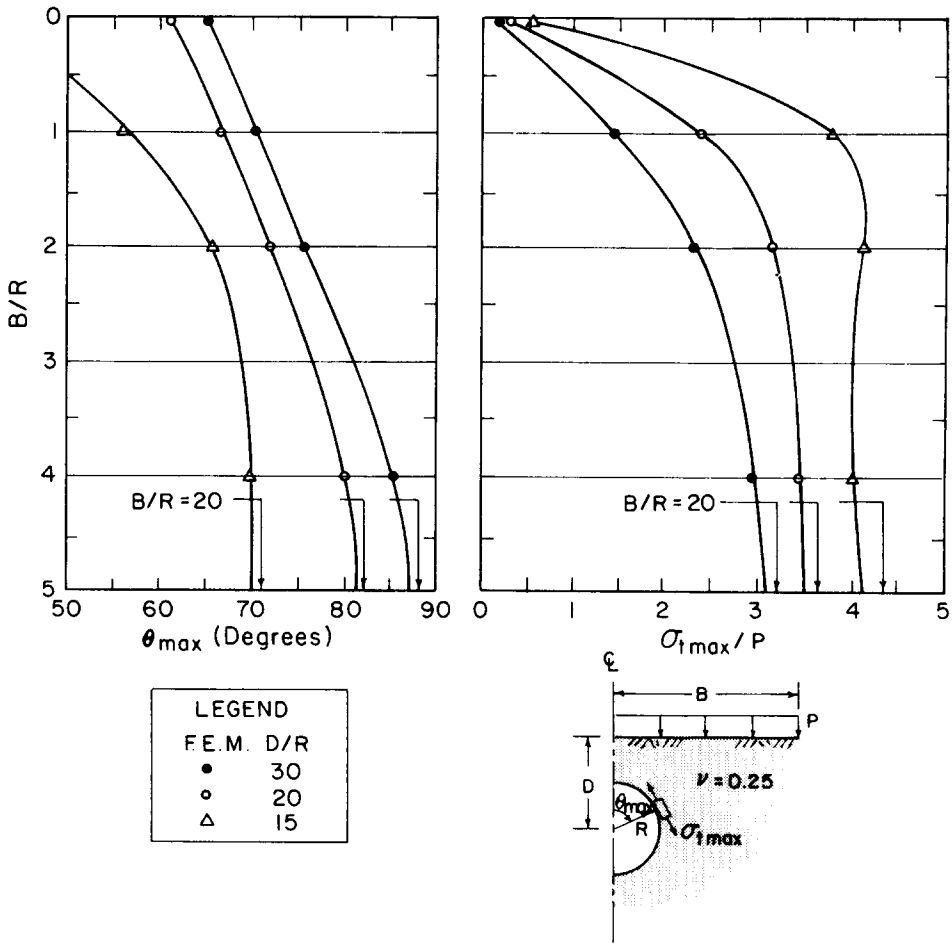

Fig. 12. The effect of the width of loading on the location and value of the maximum tangential stress.

other values of Poisson ratio could be obtained from Fig. 14, where this is searched for the displacement on the symmetry axis.

A summarizing plot for the analysis of the effect of the rigid base on surface displacements is also presented in Fig. 15. It has been noted that although the form of the settlement curves are not effected by rigid base, the amount of settlements are considerably altered.

With the use of these figures it is possible to have a first approximation to settlements on the ground surface in case where the medium could be assumed to be fairly homogenous, isotropic and linearly elastic. Variations from such properties would require modelling and analysis pertaining to the specific subsurface geological features and geotechnical engineering parameters.

6. SUMMARY AND CONCLUSIONS

In order to obtain the first approximations to the generalized and simplified problems of engineering, the theory of elasticity provides the solutions if boundary conditions make the solution possible. In cases where the boundary conditions or material proper-

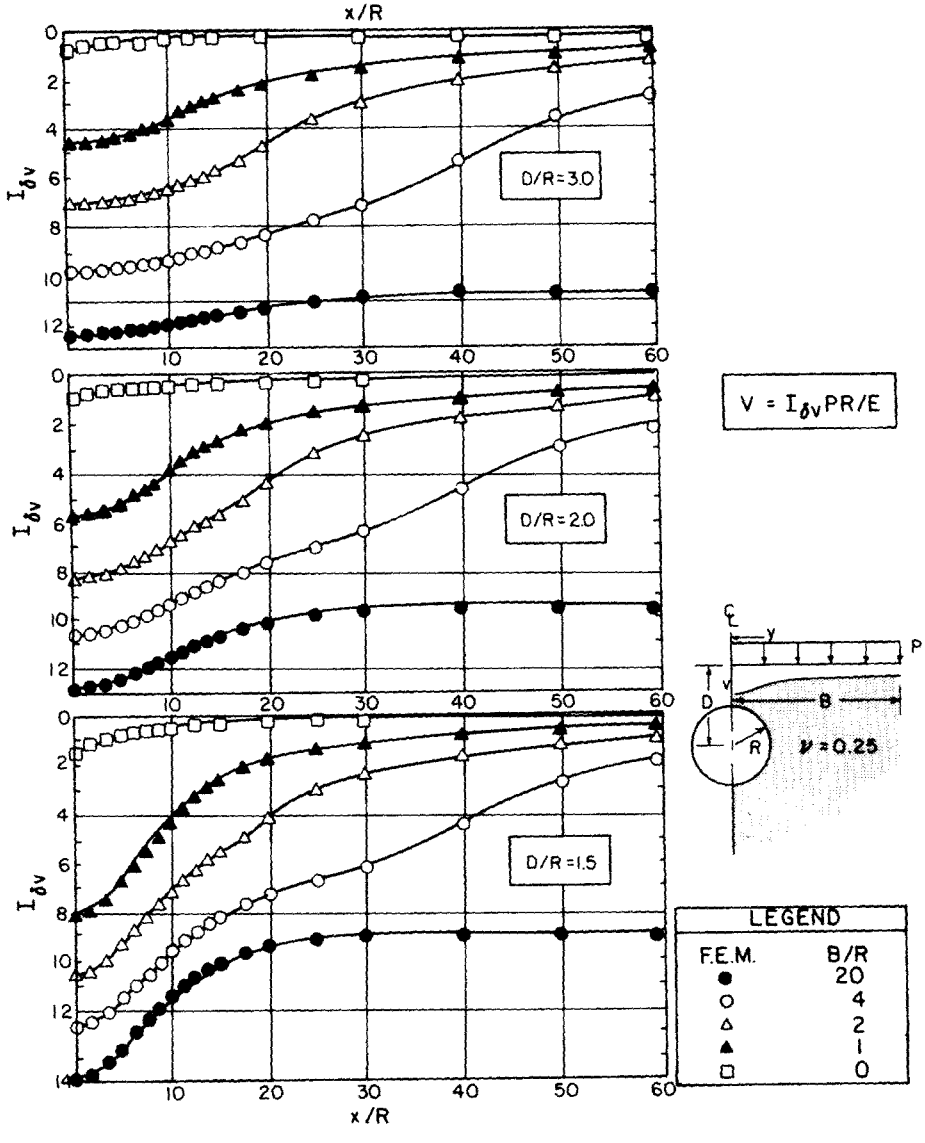

Fig. 13. The effect of loading width on the vertical displacements at the surface.

ties become more complex, numerical solutions as the finite element method are preferred after a proper discretization and modelling of the medium.

The solution for stresses and displacements to the case of a single circular opening in semi-infinite mass with uniform surface loading is investigated. The bipolar coordinate system is chosen to ease these solutions. The orthogonal transformation matrices are presented together with the stress functions from which the solutions for displacements stresses and strains are obtained.

Numerical evaluations show that the stresses diverge from the limiting case of a single circular opening in infinite medium when $D/R \leq 3.0$ and

$$y/R \leq D/R + 2.0 \tag{14a}$$

$$x/R \leq 5.0. \tag{14b}$$

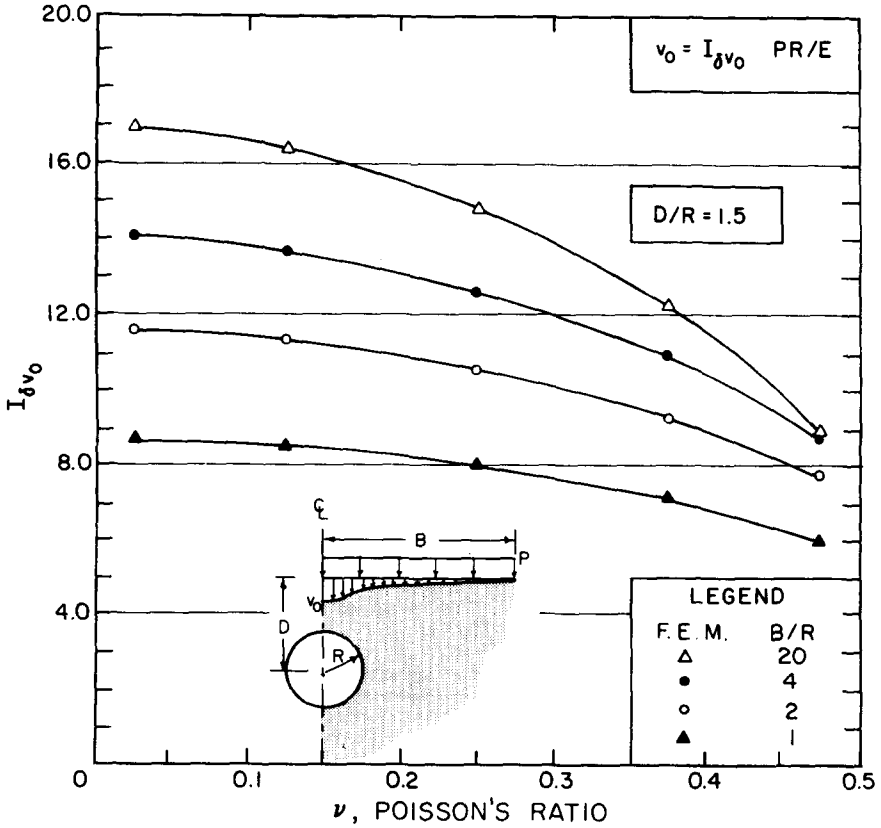

Fig. 14. The effects of the Poisson ratio on the maximum surface displacement for different B/R ratios.

Analysis of strains around the opening indicate that major displacements mainly depend upon the material properties of the medium immediately in the vicinity of the opening. As to the displacement on the ground surface it is determined that differential settlements of importance occur at a horizontal distance of

$$x/R \leq 2.0D/R \tag{15}$$

The elastic settlements on the ground surface could be obtained from the presented figures.

The effect of width of loading on the surface is parametrically analyzed by the finite element method. The semi-infinite space was properly discretized pertaining to a parametric analysis. It is observed that finite loading decreases the tensile stresses at the crown. The compressive stresses at the springings increase in value and the location of maximum concentration moves toward the crown as the opening comes close to the surface. The effect of finite loading and rigid base on the settlements on the ground surface is further analyzed and it is observed that finite loading would favor differential settlements. The results are presented in figures where pertaining specific engineering applications could easily be considered.

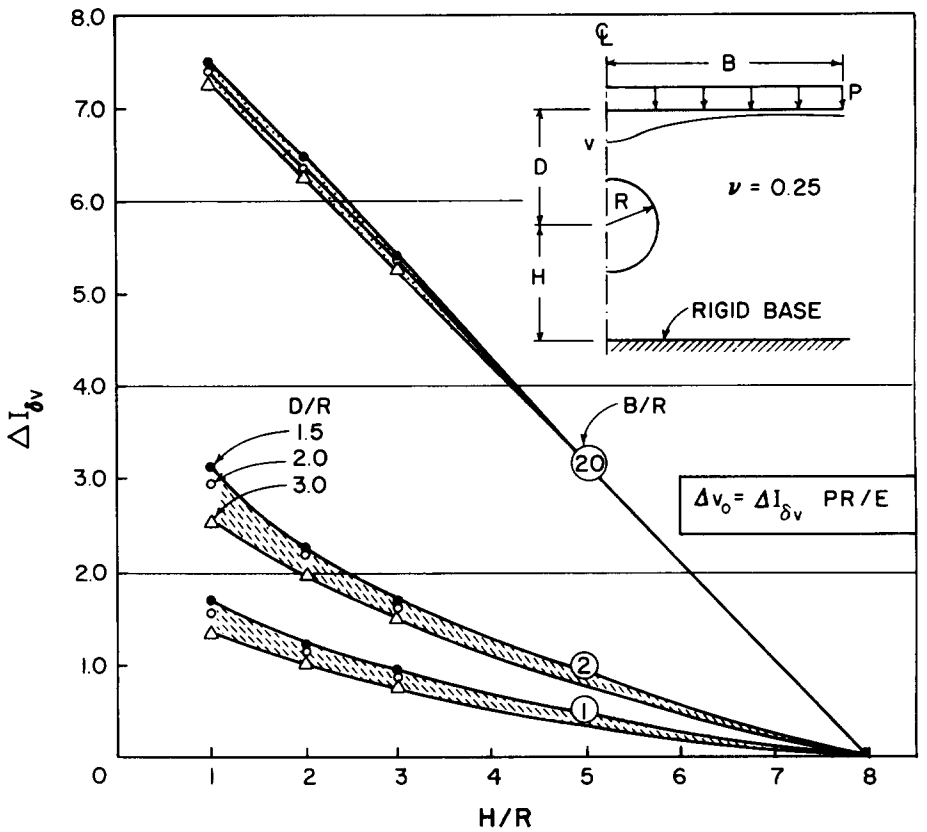

Fig. 15. The effect of rigid base to the displacement at the symmetry axis.

Acknowledgements—This study was conducted at Bogazici University, Istanbul, Turkey. Financial support obtained from the Earthquake Engineering Research Institute of this University is gratefully acknowledged.

REFERENCES

1. H. Edwards, Stress concentrations around spheroidal inclusions and cavities. *J. Appl. Mech.* **March** (1951).
2. R. Fenner, Study of ground pressures, NCR Div. of Building Research, Ottawa (1940).
3. L. Rendulich, Spannungzustand in der Umgebung eines Hohlraumes, Wasser Wirtschaft 168 (1934).
4. J. Schmied, *Statische Probleme des Tunnels—und Druckstollenbaues*, Springer, Berlin (1926).
5. K. Szechy, *The Art of Tunnelling*, Akademiai Kiado, Budapest (1967).
6. I. Szilvagyi, Die Bestimmung der Spannungen um einen Kreisformigen Tunnel, Proc. Int. Conf. Soil Mech., Budapest (1963).
7. K. Terzaghi and F. E. Richart, Jr., Stresses in rock around cavities. *Geotechnique* III, No. 3, 57–90. (1950).
8. R. D. Mindlin, Stress distribution around a tunnel, American Society of Civil Engineers, pp. 619–642 (1939).
9. Timoshenko and Goodier, *Theory of Elasticity*, McGraw-Hill, New York (1951).
10. G. B. Jeffrey, Plane stress and plane strain in bipolar co-ordinates, *Phil. Trans. R. Soc. London Sec. A* **221**, 265–293 (1921).
11. J. H. A. Brahtz, Discussion on the stress distribution around a tunnel by R. D. Mindlin. *ASCE Trans.* **105**, 1143–1151 (1940).
12. E. G. Coker and L. N. G. Filon, *A Treatise on Photoelasticity*, 2nd Ed., Cambridge University Press, Cambridge (1957).
13. Y. Acar, Circular openings in semi-infinite media, Ph.D. Dissertation, Bogazici University, Istanbul, Turkey. (1980).
14. R. W. Clough and R. S. Woodward, Analysis of embankment stresses and deformations, *J. Soil Mech. Foundation Div. ASCE* **93**, No. SM4 (1967).

15. W. D. Carrier, III and J. T. Christian, Rigid circular plate resting on a non-homogenous elastic half-space. *Geotechnique* **23**, 67–68 (1973).
16. J. M. Duncan and R. E. Goodman, Method of analysis for rock slopes, Report No. TE-68-1, University of California, Berkeley (1968).
17. H. T. Durgunoglu, Silindirik Tanklar Altindaki Gerilme ve Deformasyon Dagilimlari, Docentlik Tezi, Bogazici Universitesi (in Turkish) (1976).